3D Scan Registration using Curvelet Features in Planetary Environments

Siddhant Ahuja*, Peter Iles**, Steven L. Waslander***

*University of Waterloo, Canada
e-mail: s3ahuja at uwaterloo.ca

**Neptec Design Group, Canada
e-mail: pjwiles at neptec.com

***University of Waterloo, Canada
e-mail: stevenw at uwaterloo.ca

Abstract

Topographic mapping in planetary environments relies on accurate 3D scan registration methods. However, most registration algorithms such as ICP, GICP and NDT show poor convergence properties in these settings due to the poor structure of the Mars-like terrain and variable resolution, occluded, sparse range data that is hard to register without some a-priori knowledge of the environment. We recently proposed a novel approach to scan registration using the *curvelet transform* for topographic mapping, and in this work are demonstrating its effectiveness using simulated scans from Neptec Design Group's IVIGMS 3D laser rangefinder. At the start of the mission, the rover generates a sparse local map, and uses dense scan data while traveling to match to the original map. Simulation results comparing the average root-mean-squared errors in translation and rotation for existing methods as well as proposed approach demonstrate the improved performance of our algorithm in the challenging sparse Mars-like terrain.

1 Introduction

Motivated by the establishment of permanent presence on extraterrestrial surfaces, detailed and accurate mapping of the terrain and rover localization with respect to the environment is essential to conduct operations such as exploration, site selection, base construction etc. Without a costly absolute positioning system such as GPS available in space, on board sensing must be used for localization and mapping. The use of 3D laser scan data for planetary exploration has been proposed by numerous researchers [1, 2, 3], as a means to improve on existing stereo methods in generating detailed 3D map data, localizing over long distances and operating in low ambient light conditions. These advantages have led agencies to pursue numerous next generation rover technologies with LIDAR sensing at the core of the autonomy packages.

One of the challenges with most LIDAR sensor con-

Figure 1. IVIGMS LIDAR (white box on top of the rover mast) on the Juno rover at CSA Mars Yard in 2012.

figurations is that the needs for rover autonomy are somewhat contradictory: exploration requires rapid update over long ranges, while detailed mapping requires high densities of local points with minimal uncertainty. Neptec Design Group has recently developed the IVIGMS LIDAR sensor for the Canadian Space Agency (see Figure 1), which can be reconfigured on the fly to produce both long range sparse point clouds and short range high density clouds with the same sensor, as depicted in Figure 2 . This unique flexibility makes the IVIGMS LIDAR an interesting option for planetary navigation.

Overlapping laser scans share a common set of points that can be used for matching in order to estimate the relative rigid body transformation between scans (6-DOF rotation and translation). Separate views of the same environment can be accumulated into a global coordinate system which helps an intelligent mobile robot perform tasks in an unstructured environment. However, points within each scan represent samples of different surfaces within the environment, subject to the type of sensor used for
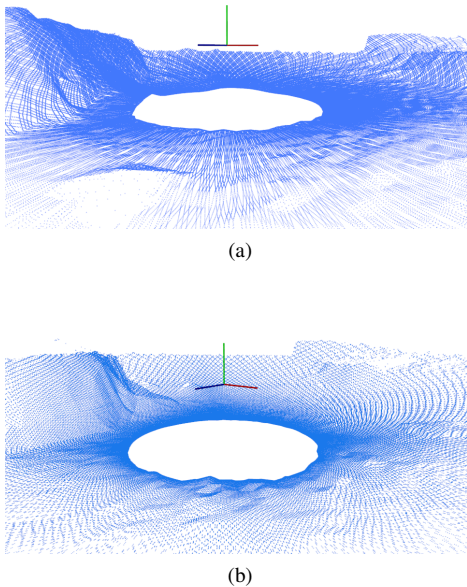
(a)

(b)

Figure 2. IVIGMS LIDAR simulated data from the CSA Mars Yard. a) Short-range dense point cloud generated over 5 seconds, b) long-range sparse point cloud generated over 20 seconds.

capturing the scene, sampling density (number of points per volumetric unit), sensor viewpoint (relative geometric position), sensitivity to measurement noise, quantization errors, occlusions, depth-discontinuities due to sharp edges, and the surface characteristics of the objects within the scene such as color, shape, textures, etc.

Finding accurate transformation parameters, given a large initial inter-scan transformation error, makes the registration problem especially hard. As demonstrated by a recent dataset collected in the University of Toronto Institute of Aerospace Studies (UTIAS) indoor rover test facility (Mars Dome) [1], mapping in an emulated Mars terrain is quite challenging as some laser scans lack sufficient features to match the scans with each other, even with full $360 \times 180°$ degree scans of the terrain with a Hokuyo laser sensor. The poor structure of the Mars like terrain coupled with the shallow grazing angle results in a variable resolution, occluded, sparse range data that is hard to register without some a priori knowledge of the environment.

Instead of working in the metric space of the laser scan, transform-based scan registration methods can often take advantage of the special properties of the transformations and improve the overall efficiency. Among various multi-scale transformations, the curvelet transform [4] is one of the many multi-resolution geometric analysis techniques that generates a sparse representation of the 3D laser scan and efficiently represents the underlying surface

structure with high anisotropic elements (edges and singularities along curves) as a set of coefficients that capture details from coarse to fine levels. The curvelet transform has been widely used in the computer vision and image processing fields for image denoising, feature extraction, edge enhancement, and image fusion, among others.

Due to the lack of natural and man-made features such as trees and buildings, most registration algorithms such as ICP, GICP and NDT show poor convergence properties. In recent work [5], we presented a novel approach to scan registration using the *curvelet transform* for topographic mapping. Instead of using an approximate sub-band of curvelet coefficients to solve the dimensionality problem, we instead found suitable features via a sum of difference of curvelets operator at multiple scales in range images. These features along with descriptors were used to calculate an approximate alignment between the scans using singular value decomposition. In this paper, we intend to improve upon this novel approach of scan registration and adapt it for the hybrid IVIGMS scanner. The IVIGMS 3D laser scanner is tuned with a set of pre-programmed beam trajectories. At the start of the mission, the rover generates a sparse local map, and uses high rate dense scan data while traveling to match to the original map and track the progress. Experimental results comparing the average root-mean-squared errors in translation and rotation for existing methods as well as proposed approach demonstrate the performance of our algorithm in the challenging sparse Mars-like terrain using the IVIGMS 3D scanner.

The rest of the paper is organized as follows: Section 2 provides the related work in the area of scan registration and a problem formulation is presented in Section 3. Details of the proposed method are given in Section 4. Quantitative and qualitative results for an indoor 3D laser scan dataset are provided in Section 5 with a discussion on suitability of the algorithm for mapping. Section 6 concludes the paper with directions for future work.

2 Previous Work

Iterative closest point (ICP) algorithm [6, 7] is widely used for scan-pair alignment by minimizing a squared-error metric between corresponding points of two laser scans. However, instead of finding salient features between the two sets of laser scans, the original ICP algorithm assumes the scan-pair is approximately aligned at the initial step, and thus correspondences are established between the closest point pairs. This assumption results in poor convergence properties of ICP, especially when there is a large inter-scan transformation error. Instead of minimizing the distance between point-pairs, Chen et. al [8] introduced the point-to-plane metric which minimizes the error between the reference point and the tangent plane of the corresponding target point. Although it has better

convergence properties than the original ICP algorithm, there is no closed-form solution for the minimization and thus relies on non-linear optimization methods. It is comparatively slower and like ICP, it relies on a good initial estimate of the scan-pair alignment. Many ICP variants have been proposed to offer better selection and weighting strategies for finding corresponding points [9], rejecting outliers, and restricting matches to points based on other channels such as color, normals, curvatures etc.

Alex et. al [10] combined the original ICP algorithm and the point-to-plane metric into a single probabilistic framework for registering scan-pairs called Generalized-ICP (G-ICP). Surface information from both scans is explicitly taken into account which necessitates computation of surface normals which increases the computational time for scan registration. Biber et. al proposed another probabilistic framework termed normal distributions transform (NDT) which locally models the measurement probability of a point and assigns a normal distribution to discrete cells. Due to the piece-wise smooth representation of the metric scan as Gaussian probability density functions, standard numerical optimization methods can be used to calculate the transformation error between scans. This eliminates the need to establish explicit correspondences. However, the discretization effects of gridding the metric scan result in discontinuities in the cost function that lead to poor convergence at cell boundaries [11]. To overcome this problem, many multi-scalar approaches have been proposed utilizing overlapping grids [12] and clustering [13, 14, 15].

Feature based methods rely on extraction of unique interest points from metric scans to aid in the correspondence based registration process. A wide variety of feature detectors based on color [16], curvatures [17], corners [18], planes [19], peaks [20] and slopes [21] have been proposed in the literature. Wu et. al [22] proposed a multi-feature based method combining lines, points and surface patches to register lunar topographic models. However, the feature extraction process is prone to measurement noise, occlusions and depth-discontinuities in the natural terrain.

A hybrid approach relying on the transformation of metric space to feature space was proposed by authors [5]. An optimal sparse representation of the environment is generated using Curvelet transform and curvelet features along with descriptors are used for scan-registration.

3   Problem Formulation

Two 3D points sets are defined: the model set $M = \{m_1, \cdots, m_{N_M}\}$ and the data set $D = \{d_1, \cdots, d_{N_D}\}$ where $m_i, d_j \in \mathbb{R}^3$ for $i \in \{1, \cdots, N_M\}, j \in \{1, \cdots, N_D\}$. A scan-to-scan registration algorithm seeks to identify a 6-DOF transformation of the data scan to match a model

scan coordinate frame to form a single, globally consistent model of the environment. This is done by maximizing the similarity between scans after transformation. An estimate, T, of the transformation $T^* = \{R, t\} \in \mathbb{SE}(3)$, with rotation $R = \{R_x, R_y, R_z\} \in \mathbb{SO}(3)$ and translation $t = \{t_x, t_y, t_z\} \in \mathbb{R}^3$ can be obtained from:

$$T^* = \underset{T \in \mathbb{SE}(3)}{\operatorname{argmax}} \; C(M, T(D)) \qquad (1)$$

where $C(M, T(D))$ is the similarity metric between the model set M and the transformed data set $T(D)$.

4   Proposed Method

The curvelet based registration method employed in this work was first presented recently by the authors in [5]. The details of the algorithm are included here for completeness. The method defines a similarity metric via a five-part algorithm as follows.

First, range images R_M and $R_D \in I = \mathbb{R}_+^{X \times Y}$ of dimension $X \times Y$ are constructed from the spherical projections of the 3-D laser scans, M and D, respectively. Hole filling is used to remove background regions surrounded by a connected border of foreground pixels [23]. Gaussian smoothing and normalization are then applied to the range values. Figure 3 shows the range image generated from the first 3D laser scan in the simulated CSA Mars emulation terrain dataset, with an angular resolution of 0.5 degrees in both x and y directions.
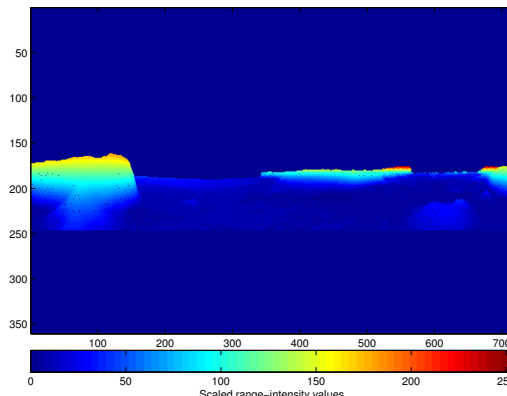

Figure 3. Range image generated from the spherical projection of the seventeenth 3D laser scan in the simulated CSA Mars emulation terrain dataset, with an angular resolution of 0.5 degrees in both x and y directions.

Next, each range image is passed through a discrete curvelet transform, which results in two sets of curvelet coefficients. The discrete curvelet transform is a linear

digital transformation which generates curvelet parameters $c(j, k, l)$ parameterized in scale (j), orientation (l) and position (k) (see [4] for details). The curvelet transform has been implemented using a second generation fast discrete curvelet transform (FDCT) via wrapping, and is available at http://www.curveleab.org. Figure 4 presents the log of the curvelet coefficients for the range image in Figure 3 for scales from the coarsest to level 4, and for angles from the 2nd coarsest to level 16. The center of the display shows the low frequency coefficients at the coarsest scale, with the Cartesian concentric coronae at the outer edges at various scale levels, showing coefficients at higher frequencies. Each corona contains four strips which are subdivided into angular panels [4]. The
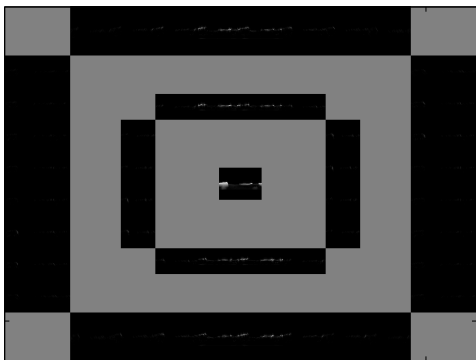

Figure 4. Log of the curvelet coefficients for the range image in Figure 3 for $\lambda = 1 \ldots 4$ and $\phi = 2 \ldots 16$.

Cartesian array formed from the range image can be exactly reconstructed from the curvelet coefficients $c(j, l, k)$ by taking the inverse curvelet transform as defined in [4]. It is also possible to construct inverse images at each scale level individually, allowing for separation of large scale and small scale structures. Denote each scale dependent reconstructed image as $I_c(j)$, where j denotes the scale used to create the image.

The proposed method then proceeds to define a difference of curvelets image, by subtracting different reconstructed scale images at nearby scale bands as follows:

$$I_{DoC}(j) = I_c(j) - I_c(j - 1) \qquad (2)$$

As is common in feature extraction methods such as the Scale Invariant Feature Transform (SIFT) [24], we identify robust local minima and maxima with high contrast over adjacent difference of curvelets images . The remaining points are then used as feature points, for which a descriptor is defined using a standard 3D histogram of image gradients. The resulting features are presented in Figure 5.

Once features and descriptors have been established for each scan, approximate nearest neighbor search is per-
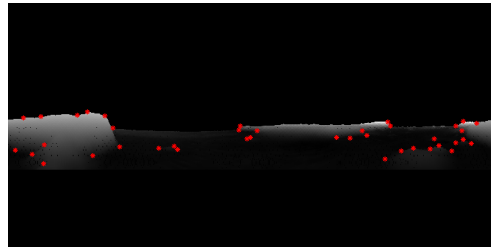

Figure 5. Curvelet features (in red) from the range image in Figure 3.

formed in the descriptor space and RANSAC is applied to reduce the effect of failed correspondences. Finally, it is possible to determine a coordinate transformation between the two scans using singular value decomposition.

5 Experimental Results

The proposed approach is evaluated using a planetary analogue outdoor simulated dataset consisting of 40 scans obtained by simulating the IVIGMS laser rangefinder, as depicted in Figure 6. The scans were taken from the simulated CSA Mars emulation terrain, for which a digital elevation map (DEM) of dimensions 60m x 120m at 25cm resolution was made available.
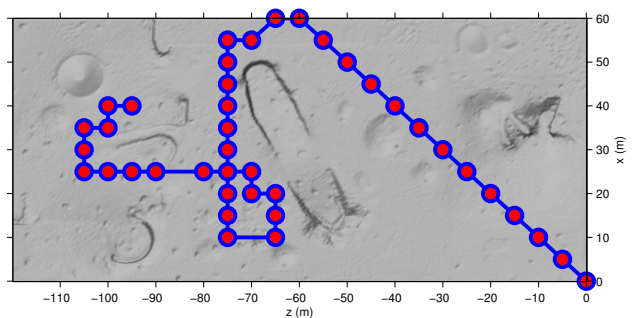

Figure 6. Overhead view of the CSA Mars emulation terrain and the rover scan locations.

The emulation terrain includes unstructured Mars-like surface elements constructed of sand and gravel, and containing ridges, hills and a crater. Registering scans from the emulated Mars terrain is quite challenging as some laser scans demonstrate low degree of overlap and lack sufficient features to match the scans with each other. The poor structure of the Mars like terrain coupled with the shallow grazing angle of the laser scanner results in a variable resolution, occluded, sparse range data set that is hard to register without some a-priori knowledge of the envi-

ronment. Ground truth data consists of absolute sensor pose data provided by the IVIGMS simulator.

The algorithms used for comparison are ICP, G-ICP, and NDT, with reference implementations provided in the point-cloud library (PCL) [25]. The ICP and G-ICP are implemented with maximum correspondence distance set to 10m, and the NDT algorithm is implemented with New-ton line search maximum step length of 0.1, and voxel grid resolution of 2m. For all algorithms, the maximum itera-tions was set to 500 and the optimization was terminated when the norm of the gradient or the norm of the step size falls below 10^{-6}.
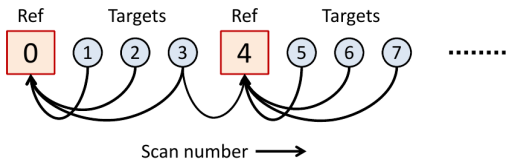

Figure 7. Scan matching is performed be-tween every fourth scan as a reference and one preceding and three consecutive scans as targets.

Pair-wise scan registration was performed between every fourth scan as a reference and one preceding and three consecutive scans as targets, with initial conditions set to zero (see Figure 7). The rotation and translation transformation is compared with the ground truth mea-surements to produce absolute error for each registration and is presented in empirical distribution function plot form in Figure 8.

The errors distributions in Figure 8 demonstrate that the proposed curvelet algorithm converges faster to a max-imum probability of one, and produces the most consis-tently accurate results than ICP, GICP and NDT. In fact, from a registration perspective, errors in rotation in ex-cess of 0.5 rad can be considered registration failures. Al-though some failures could to be detected and/or rejected by robust back-end loop closure techniques such as [26], it is preferable to avoid such failure in scan-to-scan reg-istration in the first place. Figure 9 shows the final dense map generated by integrating all registered scans for the proposed method, and the first five aligned scans for the G-ICP method. Errors in translation and rotation from the G-ICP method result in a mis-aligned map, whereas the proposed method produces an accurate dense map of the CSA Mars emulation terrain.

Figure 10 displays the close-up views of the fifth reg-istered scan-pair using ICP, G-ICP, NDT, and curvelet methods. It is possible to observe that the resulting ag-gregated pair of registered scans using the curvelet algo-rithm demonstrate better alignment when compared with
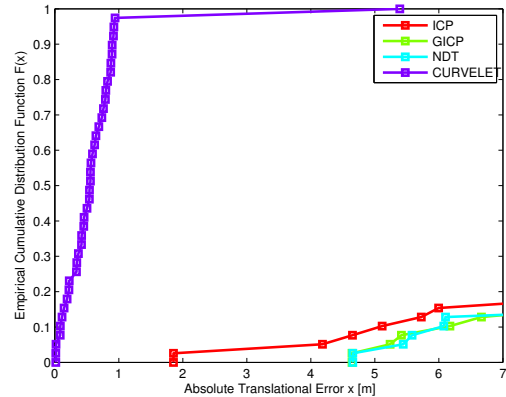
(a)
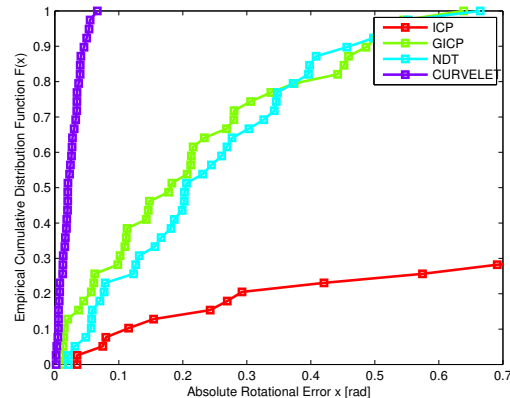
(b)

Figure 8. Empirical cumulative distribu-tion function plots for errors in trans-formation parameters for the simulated CSA Mars emulation terrain. (a) Abso-lute translational error (m). (b) Absolute rotational error (rad).

the other algorithms. In particular, the high rotational alignment accuracy is visible at the front edge of the scan in Figure 10-(f), and is less accurate in Figure 10-(c) to 10-(e). Some translational error remains in the curvelet registered pair, as visible on the left side of the scan, but this is small in comparison to the errors observed in regis-trations performed with the other three algorithms.

6 Conclusions and Future Work

This work presents the use of a curvelet transform based method for improving the convergence properties of standard registration algorithms on scans generated us-ing Neptec Design Group's IVIGMS 3D laser rangefinder. The unique feature of this sensor is its ability to scan at
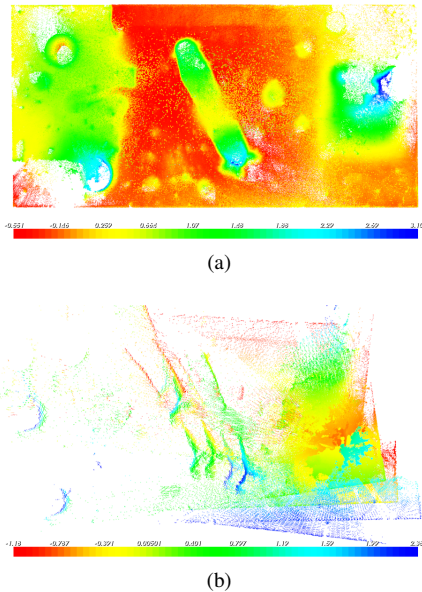
(a)

(b)

Figure 9. Final map generated by integrating registered scans (intensity scaled in y-axis from low-red to high-blue) (a) Curvelet map. (b) G-ICP map (Only aligned scans[0-4] are plotted to demonstrate the effect of errors in translation and rotation in building a dense map).

(a)

(b)

(c)

(d)

(e)

(f)

Figure 10. Registered laser scans 4 (green) and 5 (red) from simulated CSA Mars emulation terrain, (a) No alignment (b) Ground Truth (c) ICP (d) GICP (e) NDT (f) Proposed Method. (best viewed in colour)

different ranges and with different scan patterns. We exploit this characteristic by registering small local scans to a large long range scan and demonstrate using simulation results that most existing scan registration methods fail on planetary analogue terrain with scans of different point densities and with significant occlusion effects and weakly defined geometric features. The curvelet registration method proposed continues to perform reliably in simulation despite these difficulties, and represents an interesting approach for robust registration in challenging environments.

References

[1] C. H. Tong, D. Gingras, K. Larose, T. D. Barfoot, and E. Dupuis, "The canadian planetary emulation terrain 3d mapping dataset," *The International Journal of Robotics Research*, vol. 32, no. 4, pp. 389–395, 2013.

[2] P. J. F. Carle, P. T. Furgale, and T. D. Barfoot, "Long-range rover localization by matching lidar scans to orbital elevation maps," *J. Field Robot.*, vol. 27, no. 3, pp. 344–370, May 2010.
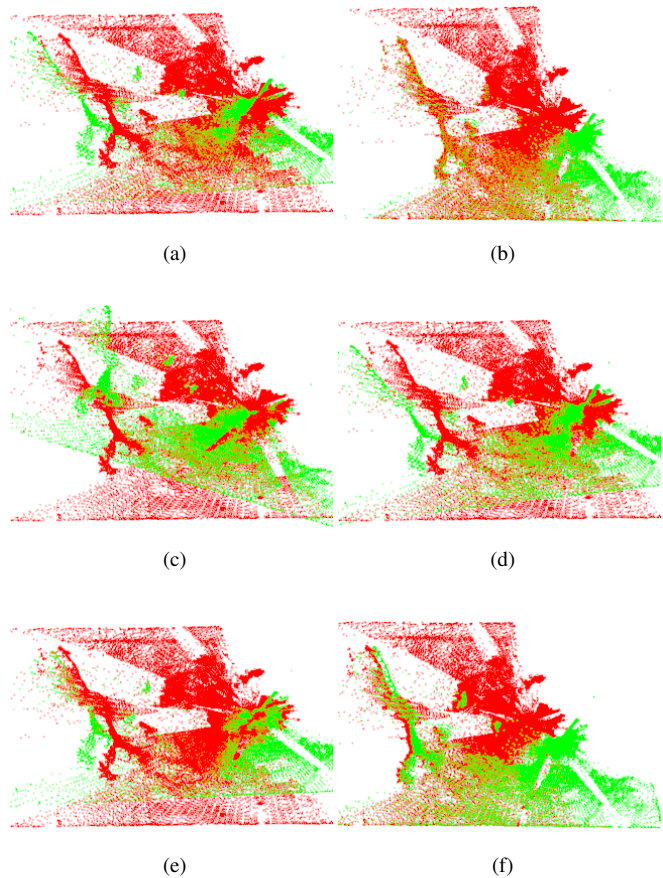
[3] J.-F. Hamel, M.-K. Langelier, M. Alger, P. Iles, and K. MacTavish, "Design and validation of an absolute localization system for the lunar analogue rover "artemis"," in *11th International Symposium on Artificial Intelligence, Robotics and Automation in Space*, Turin, Italy, 2012.

[4] E. Cands, L. Demanet, D. Donoho, and L. Ying, "Fast discrete curvelet transforms," *Multiscale Modeling and Simulation*, vol. 5, no. 3, pp. 861–899, 2006.

[5] S. Ahuja and S. L. Waslander, "3d scan registration using curvelet features," in *to appear in Canadian Conference on Computer and Robot Vision*, Montreal, QC, Canada, May 2014.

[6] P. J. Besl and N. D. McKay, "A method for registration of 3-d shapes," *IEEE Transactions on Pattern Analysis and Machine Intelligence*, vol. 14, no. 2, pp. 239–256, February 1992.

[7] Z. Zhang, "Iterative point matching for registration of free-form curves and surfaces," *International Journal of Computer Vision*, vol. 13, no. 2, pp. 119–152, October 1994.

[8] Y. Chen and G. Medioni, "Object modeling by registration of multiple range images," in *Proceedings of IEEE International Conference on Robotics and Automation (ICRA)*, vol. 3, Sacramento, CA, USA, April 1991, pp. 2724–2729.

[9] C. Dorai, J. Weng, and A. Jain, "Optimal registration of object views using range data," *IEEE Transactions on Pattern Analysis and Machine Intelligence,*, vol. 19, no. 10, pp. 1131–1138, October 1997.

[10] A. Segal, D. Haehnel, and S. Thrun, "Generalized-icp," in *Proceedings of Robotics: Science and Systems (RSS)*, vol. 25, Seattle, WA, USA, June 2009, pp. 26–27.

[11] M. Magnusson, "The three-dimensional normal-distributions transform – an efficient representation for registration, surface analysis, and loop detection," Ph.D. dissertation, Orebro University, December 2009.

[12] M. Magnusson, A. Nuchter, C. Lorken, A. Lilienthal, and J. Hertzberg, "Evaluation of 3d registration reliability and speed - a comparison of icp and ndt," in *IEEE International Conference on Robotics and Automation (ICRA)*, Kobe, Japan, May 2009, pp. 3907–3912.

[13] A. Das and S. Waslander, "Scan registration with multi-scale k-means normal distributions transform," in *IEEE/RSJ International Conference on Intelligent Robots and Systems (IROS)*, Vilamoura, Algarve, Portugal, October 2012, pp. 2705–2710.

[14] A. Das, J. Servos, and S. Waslander, "3d scan registration using the normal distributions transform with ground segmentation and point cloud clustering," in *Proceedings of IEEE International Conference on Robotics and Automation (ICRA)*, Karlsruhe, Germany, May 2013, pp. 2207–2212.

[15] S. Ahuja and S. L. Waslander, "Scan registration using the normal distributions transform with region growing clustering for point-sampled 3d surfaces," in *AIAA Guidance, Navigation, and Control Conference*, National Harbor, MD, United States, January 2014.

[16] G. Godin, M. Rioux, and R. Baribeau, "Three-dimensional registration using range and intensity information," in *Proceedings of the SPIE: Videometrics III*, vol. 2350.   Boston, Massachusetts, USA: SPIE, November 1994, pp. 279–290.

[17] C. S. Chua and R. Jarvis, "3d free-form surface registration and object recognition," *International Journal of Computer Vision*, vol. 17, no. 1, pp. 77–99, January 1996.

[18] A. Censi, L. Iocchi, and G. Grisetti, "Scan matching in the hough domain," in *Proceedings of the IEEE International Conference on Robotics and Automation (ICRA)*, Barcelona, Spain, April 2005, pp. 2739–2744.

[19] I. Sipiran and B. Bustos, "A robust 3d interest points detector based on harris operator," in *Proceedings of the 3rd Eurographics conference on 3D Object Retrieval*, ser. EG 3DOR'10.   Aire-la-Ville, Switzerland, Switzerland: Eurographics Association, May 2010, pp. 7–14.

[20] C. H. Tong, T. Barfoot, and E. Dupuis, "3d slam for planetary worksite mapping," in *IEEE/RSJ International Conference on Intelligent Robots and Systems (IROS)*, Sept 2011, pp. 631–638.

[21] D. Streutker, F. Nancy, and R. Shrestha, "A slope-based method for matching elevation surfaces," *Photogrammetric Engineering and Remote Sensing*, vol. 77, no. 7, pp. 743–750, 2011.

[22] B. Wu, J. Guo, H. Hu, Z. Li, and Y. Chen, "Co-registration of lunar topographic models derived from change-1, selene, and {LRO} laser altimeter data based on a novel surface matching method," *Earth and Planetary Science Letters*, vol. 364, no. 0, pp. 68 – 84, 2013.

[23] P. Soille, *Morphological Image Analysis: Principles and Applications*, 2nd ed.   Secaucus, NJ, USA: Springer-Verlag New York, Inc., 2003.

[24] D. Lowe, "Distinctive image features from scale-invariant keypoints," *International Journal of Computer Vision*, vol. 60, no. 2, pp. 91–110, 2004.

[25] R. Rusu and S. Cousins, "3d is here: Point cloud library (pcl)," in *IEEE International Conference on Robotics and Automation (ICRA)*, Shanghai, China, May 2011, pp. 1–4.

[26] G. Grisetti, R. Kummerle, and K. Ni, "Robust optimization of factor graphs by using condensed measurements," in *IEEE/RSJ International Conference on Intelligent Robots and Systems (IROS)*, 2012, pp. 581–588.